Supporting Information

Nonlinear Mid-infrared Metasurface based on a Phase-Change Material

*Fuyong Yue[1, †], Riccardo Piccoli[1, †], Mikhail Y. Shalaginov[2, †], Tian Gu[2, 3, *], Kathleen Richardson[4], Roberto Morandotti[1, 5], Juejun Hu[2], and Luca Razzari[1, *]*

*Email: gutian@mit.edu

*Email: razzari@emt.inrs.ca

† These authors contributed equally to this work.

Section 1. Reproducibility and reversibility study of third-harmonic generation (THG) from a crystalline GSST film

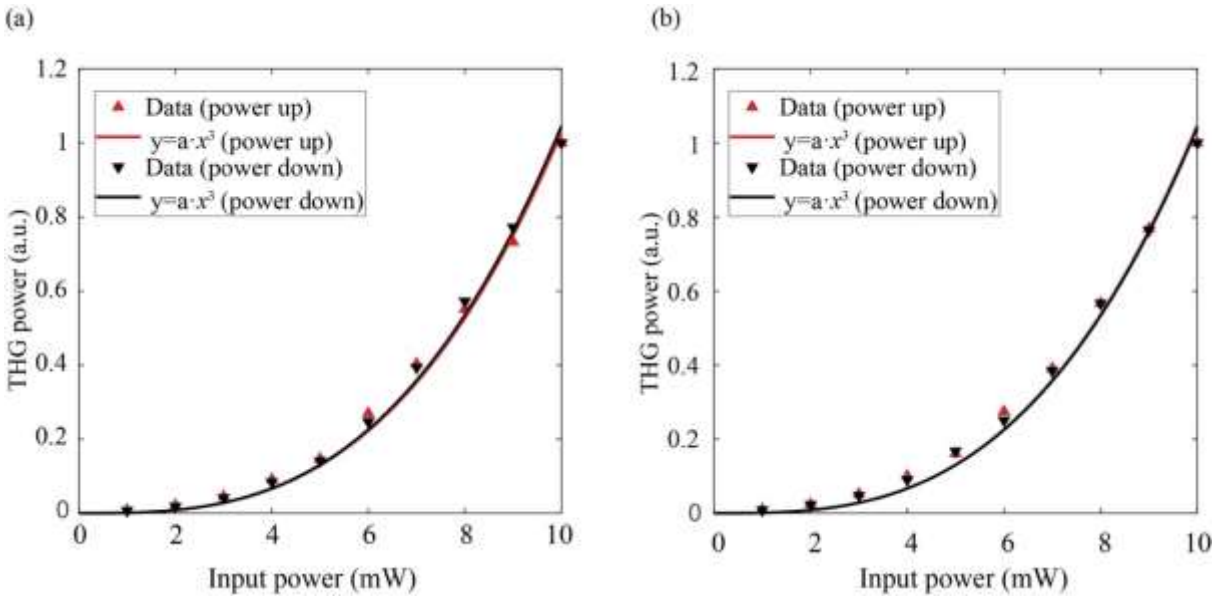

Figure. S1. Normalized experimental power dependence of THG in a crystalline GSST film. The data were collected while first increasing (red) and subsequently decreasing (black) the pump power at the fundamental wavelength of (a) 4.26 μm and (b) 4.5 μm, demonstrating the reversibility of the nonlinear response. In this case, the beam waist radius at the sample position was 120 μm.

Section 2. Estimation of $\chi^{(3)}$ from THG

Let us consider plane waves in the form of:

$$E(z,t) = A\cos(kz - \omega t) = \frac{1}{2}\left(Ae^{i(kz-\omega t)} + c.c.\right) \quad (S1)$$

where A is the electric field amplitude, $k = 2\pi n/\lambda$ is the wave vector, and ω is the angular frequency. The intensity of the plane wave is:

$$I = \frac{1}{2}\varepsilon_0 nc|A|^2 \tag{S2}$$

where ε_0 is the vacuum permittivity, n is the refractive index, and c is the speed of light.
We derived the coupled wave equations for the THG process by following the approach for the second harmonic generation:[1,2]

$$\begin{cases} \dfrac{dA_\omega}{dz} = \dfrac{3i\omega}{8n_\omega c}\chi^{(3)}A_{3\omega}A_\omega^{*\,2}e^{-i\Delta kz} \\ \dfrac{dA_{3\omega}}{dz} = \dfrac{3i\omega}{8n_{3\omega}c}\chi^{(3)}A_\omega{}^3 e^{i\Delta kz} \end{cases} \tag{S3}$$

where n_ω and $n_{3\omega}$ are the refractive indices of the pump (ω) and THG (3ω), respectively and $\Delta k = 3k(\omega) - k(3\omega)$ is the wavevector mismatch. Under the undepleted-pump approximation, where A_ω is constant, an analytical solution for the electric field amplitude $A_{3\omega}$ of the THG at the exit of a nonlinear material of thickness L can be found as:

$$\begin{aligned} A_{3\omega}(L) &= \int_0^L \frac{dA_{3\omega}}{dz}dz = \frac{3i\omega}{2n_{3\omega}c}\chi^{(3)}A_\omega{}^3 \int_0^L e^{i\Delta kz}\,dz \\ &= \frac{3i\omega}{8n_{3\omega}c}\chi^{(3)}A_\omega{}^3 L \cdot e^{i\Delta kL/2}\cdot \mathrm{sinc}(\Delta kL/2) \end{aligned} \tag{S4}$$

The intensity of THG light can be expressed as:

$$I_{3\omega} = \frac{1}{2}\varepsilon_0 n_{3\omega} c|A_{3\omega}|^2 = \left[\frac{9\pi^2\chi^{(3)^2}L^2}{4\varepsilon_0^2 n_{3\omega}n_\omega^3 c^2\lambda_p^2}\cdot sinc^2\left(\frac{\Delta kL}{2}\right)\right] I_\omega^3 = \Omega \cdot I_\omega^3 \tag{S5}$$

Therefore, the intensity-to-intensity internal THG efficiency η_I^{int} can be written as:

$$\eta_I^{int} = \frac{I_{3\omega}}{I_\omega} = \Omega \cdot I_\omega^2 \tag{S6}$$

Considering a pump beam with Gaussian profile (TEM_{00} fundamental mode), Eq. (S6) holds true if the thickness of the material is much smaller than the double Rayleigh length, i.e., $L \ll 2 \cdot z_R = \frac{2\pi w_p^2}{\lambda}$, where w_p is the beam waist defined as the distance from the beam center

to the radius where the intensity drops to $1/e^2$ of its maximum intensity. Moreover, taking into account the Gaussian temporal profile of the pump pulse (with duration τ), we have:

$$I_\omega(r,t) \equiv I_P^{int} \cdot e^{-\frac{2r^2}{w_p^2}} \cdot e^{-\frac{t^2}{\tau^2}} \qquad (S7)$$

where I_P^{int} is the internal pump peak intensity. To correlate the intensity with the average power, the previous expression has to be integrated in time and space. The energy of the pump pulse Σ_ω can be therefore calculated as:

$$\Sigma_\omega = \int I_\omega \, dAdt = \int_0^{+\infty} \int_{-\infty}^{+\infty} I_\omega \cdot 2\pi r dr dt = \frac{\pi w_p^2 \cdot I_P^{int}}{2} \sqrt{\pi}\tau \qquad (S8)$$

In a similar way, it is possible to determine the energy $\Sigma_{3\omega}$ of the THG pulse:

$$\Sigma_{3\omega} = \int I_{3\omega} \, dAdt = \int_0^{+\infty} \int_{-\infty}^{+\infty} \Omega \cdot I_\omega^3 \cdot 2\pi r dr dt = \Omega \frac{\pi w_p^2 \cdot {I_P^{int}}^3}{6} \sqrt{\frac{\pi}{3}}\tau \qquad (S9)$$

It should be noted that the THG beam waist and pulse duration are $\sqrt{3}$ times smaller than those of the pump pulse, due to the cubic dependence between the corresponding intensities. Therefore, a factor of $3\sqrt{3}$ appears in the relation between average power (or equivalently energy) and intensity internal efficiencies:

$$\eta_P^{int} = \frac{P_{3\omega}}{P_\omega} = \frac{\Sigma_{3\omega}}{\Sigma_\omega} = \frac{\Omega}{3\sqrt{3}} \cdot {I_P^{int}}^2 = \frac{\eta_I^{int}}{3\sqrt{3}} \qquad (S10)$$

In this way, it is possible to connect "real measurable" parameters (i.e., the average powers) with material parameters such as the third-order susceptibility:

$$\chi^{(3)} = \frac{2\varepsilon_0 c \lambda_p \sqrt{n_{3\omega} n_\omega^3}}{\sqrt[4]{3}\pi L I_P^{int} sinc\left(\frac{\Delta kL}{2}\right)} \sqrt{\eta_P^{int}} \qquad (S11)$$

where $I_P^{int} = I_P^{ext} \cdot T$, being I_P^{ext} the external pump peak intensity before entering the substrate, while $T = \frac{16n_{sub,\omega}^2 n_\omega}{(1+n_{sub,\omega})^2(n_\omega+n_{sub,\omega})^2}$ is the transmission of the pump beam through the CaF_2 substrate and into the film. Indeed, it is important to include the power transmission coefficients at the interfaces to calculate the effective power entering (and exiting) the samples under investigation.

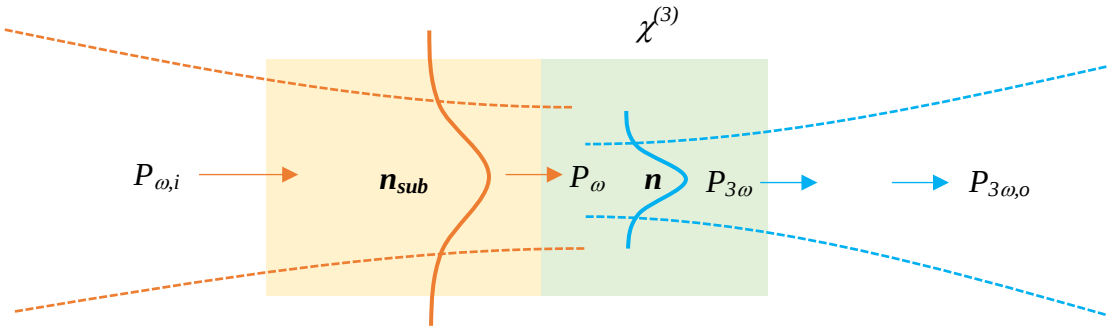

Figure S2. Schematic of THG in the samples under investigation.

Therefore, using the Fresnel coefficients for normal incidence, we obtain:

$$P_\omega = P_{\omega,i} \cdot T = P_{\omega,i} \cdot \frac{16n_{sub,\omega}^2 n_\omega}{(1+n_{sub,\omega})^2(n_\omega+n_{sub,\omega})^2} \quad (S12)$$

$$P_{3\omega,o} = P_{3\omega} \frac{4n_{3\omega}}{(1+n_{3\omega})^2} \quad (S13)$$

Finally, the "internal" power-to-power efficiency derived in Eq. (S10) can be related to the actual pump and THG powers measured at the sample's input and output, respectively (i.e. to the "external" power efficiency $\eta_P^{ext} = \frac{P_{3\omega,o}}{P_{\omega,i}}$) as:

$$\eta_P^{int} = \frac{P_{3\omega}}{P_\omega} = \eta_P^{ext} \cdot \frac{(1+n_{3\omega})^2(1+n_{sub,\omega})^2(n_\omega+n_{sub,\omega})^2}{64\, n_{sub,\omega}^2 n_\omega n_{3\omega}} \quad (S14)$$

Section 3. Generalized Miller formula

The third-order susceptibility $\chi^{(3)}$ directly connects with the THG performance of a nonlinear optical material. In order to compare the THG performance of our GSST films with other relevant nonlinear optical materials, it is necessary to project the $\chi^{(3)}$ found in literature to the same set of frequencies employed in our investigation. W. Ettoumi *et al.*

derived the spectral dependence of the nonlinear susceptibility of any order and reported a generalized Miller formula.[3] By applying such formula, the third-order susceptibilities at any set of frequencies can be estimated, if the refractive index dispersion and the nonlinear susceptibility value for a specific set of frequencies are known:

$$\frac{\chi^{(3)}_{(\omega_0:\omega_1,\omega_2,\omega_3)}}{\chi^{(3)}_{(\omega_0':\omega_1',\omega_2',\omega_3')}} = \frac{\chi^{(1)}_{(\omega_0)} \cdot \chi^{(1)}_{(\omega_1)} \cdot \chi^{(1)}_{(\omega_2)} \cdot \chi^{(1)}_{(\omega_3)}}{\chi^{(1)}_{(\omega_0')} \cdot \chi^{(1)}_{(\omega_1')} \cdot \chi^{(1)}_{(\omega_2')} \cdot \chi^{(1)}_{(\omega_3')}} \qquad (S15)$$

where $\chi^{(1)}(\omega) = n^2_{(\omega)} - 1$.

Section 4. THG performance of the crystalline and amorphous GSST films at different pump wavelengths

To further investigate the THG performance of the GSST films in crystalline and amorphous states, the power of the THG light emitted at different pump wavelengths was measured under the same experimental conditions. As we can see in Fig. S3, the conversion efficiency of the crystalline GSST film is significantly higher than that of the amorphous film over the measured pump wavelength range 4.3 μm - 4.5 μm.

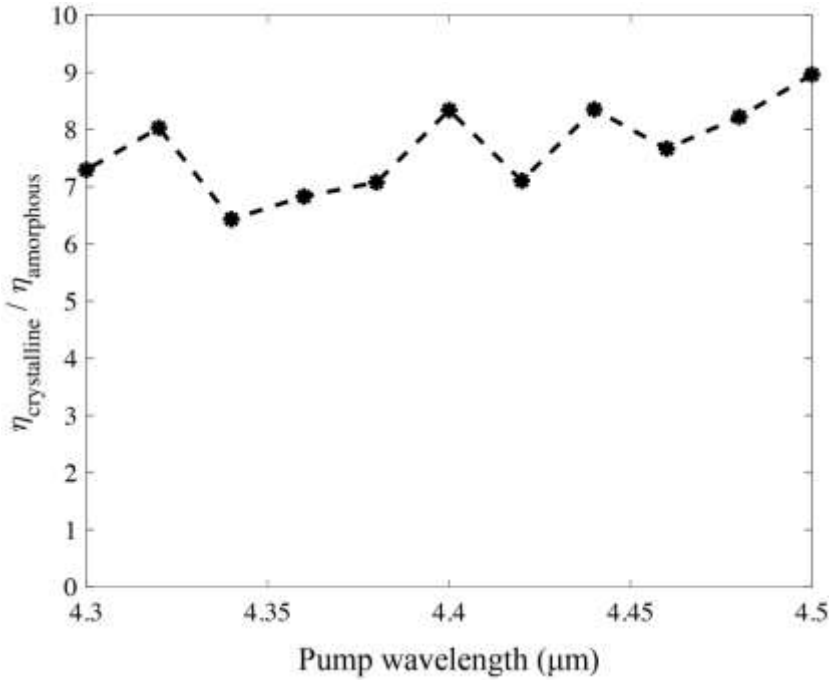

Figure S3. Ratio of the conversion efficiencies of crystalline and amorphous films at different pump wavelengths. The input average power was fixed at 9 mW and the beam waist radius was 120 μm. (The line is for visual guidance).

Section 5. Simulated transmittance of GSST cylinders with different sidewall angles

The relationship between the sidewall angle and the resonant wavelength was numerically investigated (as shown in Fig. S4). We found that a decrease in the sidewall angle (see inset in Fig. S4 for its definition) leads to a blue-shift of the magnetic dipole resonant wavelength when compared to a meta-atom with vertical sidewalls.

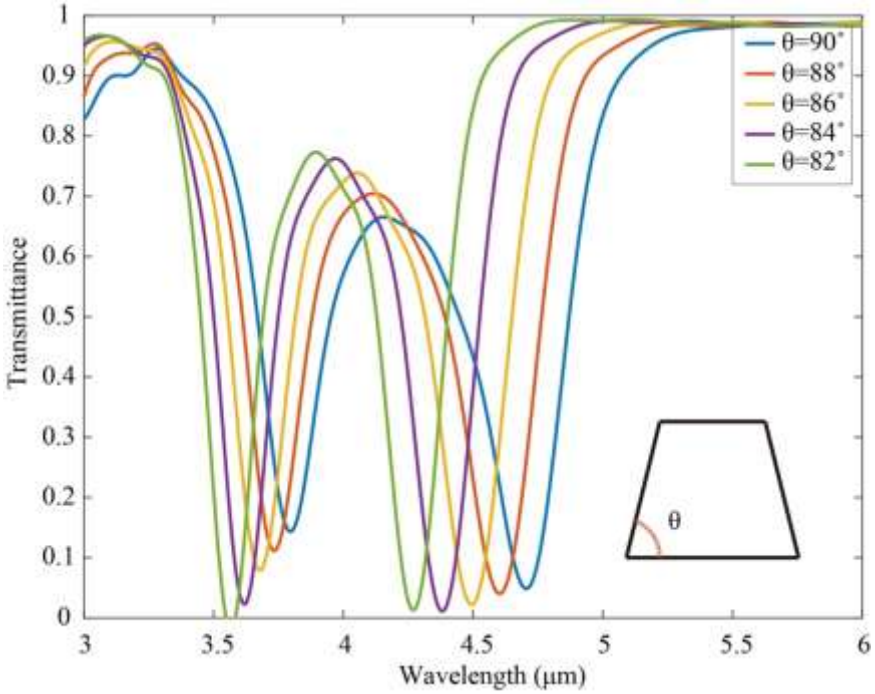

Figure S4. Simulated transmittance of GSST cylinders with different sidewall angles.

Section 6. Diffraction pattern of the THG light generated by the crystalline GSST metasurface

As reported in the main paper, the center-to-center distance between the resonant meta-atoms in the fabricated device is 2.4 μm. This corresponds to an effective sub-wavelength separation between the scatterers (as typically featured by metasurfaces [4]) for the employed mid-infrared light, considering both the air and CaF_2 substrate refractive indices. The square lattice period is instead larger than the THG wavelength, resulting in multiple diffraction orders for the generated third-harmonic light. Such condition is common in SHG/THG nonlinear experiments that employ dielectric metasurfaces with a resonance at the pump wavelength (see, e.g., Ref. [5]).

Figure S5 (b, c) shows an example of the THG light diffraction pattern generated by the metasurface (λ = 4.2 μm). Estimates of the THG power distribution over the nine diffraction

orders are provided in Fig. S5 (d). These results support the assumption that almost identical amounts of power go into each of the maxima. Consequently, we evaluated the total THG power emitted by the metasurface as the power collected from the zero-diffraction order multiplied by a factor of 9. Indeed, the THG collection from all orders was found to be experimentally challenging, especially for the longer pump wavelengths and the diagonal orders, due to their large diffraction angles (see Fig. S5 (e, f)).

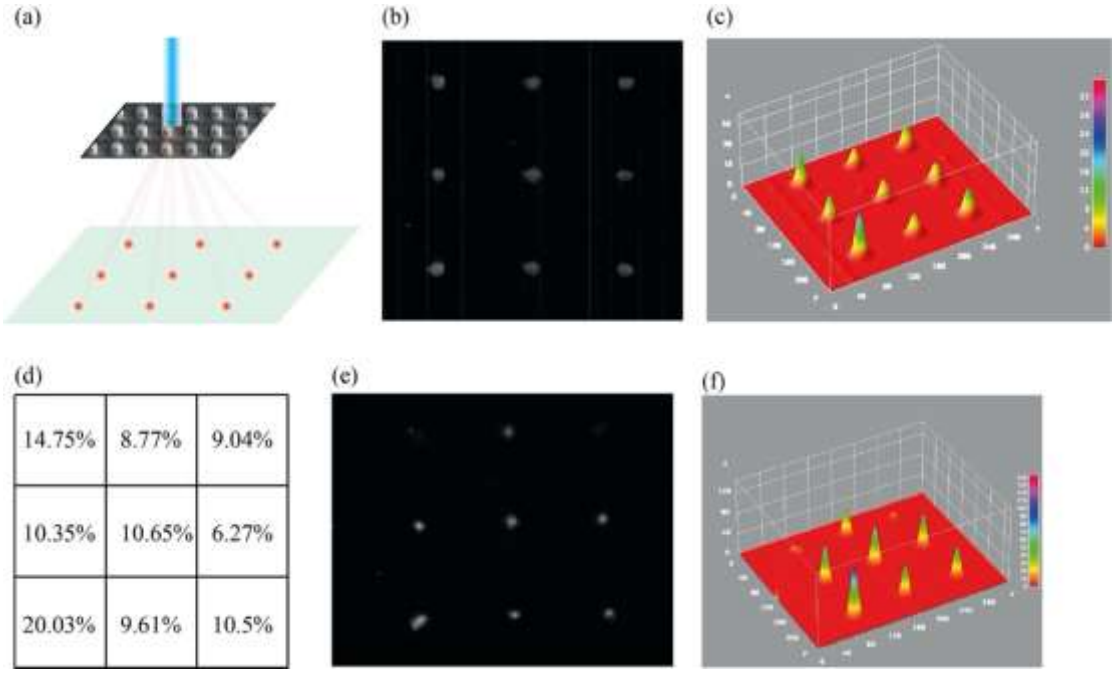

Figure S5. (a) Schematic of the diffraction pattern of the THG from the crystalline GSST metasurface. (b) Example of an experimentally recorded image of the THG diffraction pattern, corresponding to the pump wavelength of 4.2 μm. (c) Intensity profile of the diffraction pattern presented in (b). (d) Corresponding distribution of the total power over the diffraction orders (c). (e) Experimentally recorded image at the larger pump wavelength of 4.5 μm, presenting missing diagonal diffraction orders. (f) Intensity profile of the recorded diffraction pattern at 4.5 μm.

References

[1] P. S. Banks, M. D. Feit, M. D. Perry, *J Opt. Soc. Am. B* **2002**, *19*, 102.

[2] R. W. Boyd, *Nonlinear optics*, Elsevier, Berlin, Germany **2003**.

[3] W. Ettoumi, Y. Petit, J. Kasparian, J.-P. Wolf, *Opt. Express* **2010**, *18*, 6613.

[4] N. Yu, F. Capasso, *Nat. Mater.* **2014**, *13*, 139.

[5] F. J. F. Löchner, A. N. Fedotova, S. Liu, G. A. Keeler, G. M. Peake, S. Saravi, M. R. Shcherbakov, S. Burger, A. A. Fedyanin, I. Brener, T. Pertsch, F. Setzpfandt, I. Staude, *ACS Photonics* **2018**, *5*, 1786.